Multibody scattering, correlation, molecular conduction, and the 0.7 anomaly

Joseph E. Subotnik[a] and Abraham Nitzan[b]
School of Chemistry, Tel-Aviv University, 69978 Tel-Aviv, Israel

(Received 25 May 2008; accepted 2 September 2008; published online 10 October 2008)

We describe a new grid-based (or localized orbital-based) method for treating the effects of exchange and correlation on electronic transmission through a molecular target where there are initially other bound electrons. Our algorithm combines the approaches of (i) solid-state grid-based algorithms using self-energies and (ii) the complex Kohn method from electron-molecule scattering. For the general problem of a molecular target with n-electrons, our algorithm should ideally solve for electronic transmission with a computational cost scaling as n^2, although the present implementation is limited to one-dimensional problems. In this paper, we implement our algorithm to solve three one-dimensional model problems involving two electrons: (i) Single-channel resonant transmission through a double-barrier well (DBW), where the target already contains one bound-state electron [Rejec *et al.*, Phys. Rev. B **67**, 075311 (2003)]; (ii) multichannel resonant transmission through a DBW, where the incoming electron can exchange energy with the bound electron; (iii) transmission through a triple-barrier well (TBW), where the incoming electron can knock forward the bound electron, yielding a physical model of electron-assisted electron transfer. This article offers some insight about the role and size of exchange and correlation effects in molecular conduction, where few such rigorous calculations have yet been made. Such multibody effects have already been experimentally identified in mesoscopic electron transport, giving rise to the "0.7 anomaly," whereby electrons traveling through a narrow channel pair up as singlets and triplets. We expect the effect of electronic correlation to be even more visible for conduction through molecules, where electrons should partially localize into bonding and antibonding orbitals.
© *2008 American Institute of Physics*. [DOI: 10.1063/1.2988495]

I. INTRODUCTION

From a quantum mechanical perspective, the conduction of electrons through a microscopic junction is fundamentally related to the time-independent scattering states traversing the molecule. Indeed, one may describe a metal-molecule-metal junction under voltage as a molecule with large contact reservoirs of electrons on its left and right, each of which is filled up to its respective Fermi energy. According to the Landauer formula,[1,2]

$$I = \frac{2e}{h}\sum_{nm}\int_{-eV/2}^{eV/2} T_{nm}(E)dE, \tag{1}$$

the current through the molecule (I) is proportional to the difference in transmission (T_{nm}) for electronic currents going in different directions through the junction with incoming channel n and outgoing channel m. (Here V is the voltage window.) Thus, in order to calculate the low bias conduction of a molecule, one needs to compute the transmission function $T(E)$, where E is the kinetic energy of the incoming electron.

Several methods have been advanced for calculation of this transmission function. Almost always, these have single electron character in which the effects of wave function antisymmetry (i.e., "exchange") and correlation are either ignored or treated on a mean-field level. The error incurred when approximating these effects for transmission calculations is difficult to estimate most generally, but quantum chemistry calculations for molecules in bound states indicate that these effects can be crucial. Abundant research on molecules in the gas phase confirms that without properly accounting for exchange and correlation, ground-state and excited-state energies cannot be obtained to within chemical accuracy. Exchange and correlation are also important for accurate descriptions of low-energy electron-scattering experiments. Indeed, current state-of-the-art algorithms for doing three-dimensional electron scattering must account for exchange and correlation for chemical accuracy. This is done in different ways for the different three-dimensional electron-scattering approaches (e.g., the complex Kohn method,[3–5] the Schwinger multichannel method,[6] and the R-matrix method[7]). In this paper, we will borrow slightly from the complex Kohn method. According to the Kohn method, one introduces a basis consisting of Gaussian atomic orbitals near the molecule and free waves emanating from the center of the molecule, and then one uses this basis to construct a scattering wave function. By antisymmetrizing the wave function and allowing for different bound-state channels (i.e., usually excited states) and so-called "closed-state channels"

[a]Electronic mail: subotnik@post.harvard.edu.
[b]Electronic mail: nitzan@post.tau.ac.il.

 © 2008 American Institute of Physics

Author complimentary copy. Redistribution subject to AIP license or copyright, see http://jcp.aip.org/jcp/copyright.jsp

(i.e., channels that that do not change the asymptotic state of the outgoing scattering electron), the complex Kohn method accounts for exchange and correlation.

Focusing on the electron transmission problem, there is growing evidence that state of the art calculations based on mean-field theories (including density functional theory) fail to account quantitatively and sometimes qualitatively for many physical observations and can be very sensitive to the exchange-correlation functional (e.g., see Ref. 8). Different techniques have thus far been introduced for including electron-electron correlation with varying degrees of success. Techniques based on Green's functions and perturbation theory have been introduced by Ortiz and co-workers,[9,10] techniques based on Green's functions and clever construction of self-energies by Feretti *et al.*,[11,12] techniques based on functional renormalization group theory by Meden and co-workers,[13–15] and techniques based on constraining the Wigner transform by Delaney and Greer.[16] This list is by no means exhaustive.

In this paper, we focus on the Landauer formula for current. Even though the Landauer formula is usually derived from a mean-field one-electron model, if we assume that the incoming electron has the same energy as the outgoing electron, the Landauer formula for the current is valid using advanced electronic structure theories that go beyond the mean field (and capture electronic correlation). Thus, when calculating the elastic transmission of a single electron through a molecule, one can account for the electronic correlation near the molecular target by including degenerate bound-state channels and all closed-state channels, and subsequently plugging the result into the current formula. In Secs. II and III of this paper, we take a close look at this issue by performing an essentially exact calculation of electron transmission through a molecular target, represented by a one-dimensional double-barrier well (DBW) (first solved in Ref. 17) or triple-barrier well (TBW) that already contains another electron. For this two-electron problem, we calculate electronic transmission using a grid-based algorithm that fully takes into account the effects of exchange and correlation. We do this for both possible spin cases: The two electrons can have the same spin or opposite spins, and these two possibilities exhibit very different transmission behavior.

We use a grid-based algorithm for this two-electron problem for several reasons. First, without a scattering center, from which the scattered wave function emanates, the traditional complex Kohn method is not immediately applicable. Second, calculations based on grid points or localized orbitals should offer a means for computational savings in computing matrix elements compared to traditional electron-scattering algorithms. Third, working with a basis of spatially localized grid points allows us to assess how local are the effects of electron-electron correlation around the target.

After analyzing the two-electron problem, in Secs. IV A and IV B, we discuss more generally the role of exchange and correlation on electronic transmission and electron transfer. We do this in the context of the "0.7 anomaly"[18] of mesoscopic physics, which is usually regarded as an experimental manifestation of electron-electron correlation. Finally, in Sec. IV C, we hypothesize about an algorithm for solving the many-electron scattering problem. For the three-dimensional many-electron problem, we anticipate using localized Gaussian orbitals in lieu of one-dimensional grid points. We anticipate that, to a good approximation, the low-energy scattering problem can be solved accurately (beyond the mean-field approximation) in a computational time that scales ideally as the square of the number of electrons. Our algorithm will rely heavily on all of the tricks of local correlation theory[19] from quantum chemistry.

II. THEORY: STEADY-STATE TWO ELECTRON SCATTERING COMPUTED OVER A GRID

We seek to calculate the wave function describing an incoming electron as it attempts to pass through a molecular target, which is initially occupied by another bound electron. For concreteness, one may consider the target to be a DBW as in Fig. 2 or a TBW as in Fig. 7. The problem of one electron passing through an exactly symmetric double well (initially occupied by another electron) and with one possible outgoing channel was first solved by Rejec *et al.*[17] Our algorithm below applies to two electrons interacting in an arbitrary external potential and, in Sec. IV C, we will show the generalization to many electrons. As noted by Rejec *et al.*, there are effectively two ways to solve the two-electron dynamical problem: On the one hand, if we assume that the bound electron remains in a static single-electron orbital in the target, we recover mean-field theory. On the other hand, if we allow both electrons to interact without any constraints (so that each electron can respond to the other), we recover a correlated multielectron scattering wave function.

For simplicity, we restrict ourselves to energies low enough such that there is no chance for both the incoming and bound electrons to be released from the target. In other words, the kinetic energy of the incoming electron is always less than the binding energy of the bound-state electron. For our problem that involves two indistinguishable electrons with spin, two different levels of treatment (mean field and correlation) and two different spin cases (same spin and opposite spin) can be identified for the scattering problem, giving a total of four cases (all of which will be treated below). Note that, provided the Hamiltonian does not depend on spin, the case of spinless "distinguishable electrons" is isomorphic to the case of opposite-spin indistinguishable electrons.

A. A one-electron scattering formalism over a grid

Let us consider a Hamiltonian $H=T+V(x)$, where the potential energy $V(x)$ is assumed nonzero only in a finite region about the origin. This Hamiltonian is described on a finite uniformly spaced grid which encompasses the region of nonzero V. Fixing a as the uniform grid spacing, we construct a grid going from $-na$ to $+na$, with $2n+1$ grid points. Here, n is some integer large enough such that $V(x)=0$ for $|x|\geq na$. In what follows, we shall consider this set of grid points to be a vector space, and we shall denote the basis element at grid point i as $|g_i\rangle$. Working in this finite vector space, we seek to compute the transmission for an incoming electron. We represent the kinetic energy operator using a

Author complimentary copy. Redistribution subject to AIP license or copyright, see http://jcp.aip.org/jcp/copyright.jsp

three-point approximation for the second derivative. The matrix elements of the potential and kinetic energy operators in this basis are thus as follows:

$$V_{ij} = \delta_{ij} V(i), \tag{2}$$

$$T_{ij} = \frac{-\delta_{i,j+1} - \delta_{i,j-1} + 2\delta_{ij}}{a^2}. \tag{3}$$

Here, we work in a.u. and we take $m=1/2$ so that we may ignore the $2m$ term in the kinetic energy operator $(p^2/2m)$. The Hamiltonian H is defined by $H=T+V$ for one electron.

Our first step is to define three new vectors, which depend on the given incoming wavevector k:

$$|w_{\text{inc}}\rangle \equiv |g_{-n}\rangle + e^{ika}|g_{-n+1}\rangle, \tag{4}$$

$$|w_{\text{refl}}\rangle \equiv |g_{-n+1}\rangle + e^{ika}|g_{-n}\rangle, \tag{5}$$

$$|w_{\text{trans}}\rangle \equiv |g_{n-1}\rangle + e^{ika}|g_{n}\rangle. \tag{6}$$

All matrix elements of the $|w\rangle$ vectors can be constructed from Eq. (2).

Next, consider the vector space $Y \equiv \text{span}(g_{-n}, g_{-n+1} \cdots g_{n-1}, g_n, w_{\text{refl}}, w_{\text{trans}})$. Although we have written Y with $2n+3$ vectors, it follows from the definitions of $|w_{\text{inc}}\rangle$ and $|w_{\text{refl}}\rangle$ that $\dim(Y)=2n+1$, which is the number of grid points. In fact, it is helpful to use the decomposition $Y=Y_{\text{inner}} \oplus Y_{\text{outer}}$. Here, we define $Y_{\text{inner}} \equiv \text{span}(g_{-n+2}, g_{-n+3} \cdots g_{n-3}, g_{n-2})$ and $Y_{\text{outer}} \equiv \text{span}(g_{-n}, g_{-n+1}, g_{n-1}, g_n, w_{\text{refl}}, w_{\text{trans}})$. As should be clear, $\dim(Y_{\text{inner}})=2n-3$ and $\dim(Y_{\text{outer}})=4$.

Solving the scattering problem for an incoming wave with wavevector k amounts to solving the Schrodinger equation for $|\Psi\rangle=|w_{\text{inc}}\rangle+|v\rangle$ for $|v\rangle \in Y$.

$$H|\Psi\rangle = E_{\text{inc}}|\Psi\rangle. \tag{7}$$

We choose to solve this equation in reduced spaces $W_{\text{bra}}, W_{\text{ket}} \in Y$, where $\dim(W_{\text{ket}})=\dim(W_{\text{bra}})=2n-1$ and the W subspaces are defined as follows:

$$W_{\text{ket}} = \text{span}\{|\eta_j\rangle\} \equiv \text{span}\{|g_{-n+2}\rangle, \ldots, |g_{n-2}\rangle, |w_{\text{refl}}\rangle, |w_{\text{trans}}\rangle\}, \tag{8}$$

$$= \text{span}\{|w_{\text{refl}}\rangle, Y_{\text{inner}}, |w_{\text{trans}}\rangle\}, \tag{9}$$

$$W_{\text{bra}} = \text{span}\{\langle\phi_i|\} \equiv \text{span}\{\langle g_{-n+1}|, \langle g_{-n+2}|, \ldots, \langle g_{n-2}|, \langle g_{n-1}|\}, \tag{10}$$

$$= \text{span}\{\langle g_{-n+1}|, Y_{\text{inner}}, \langle g_{n-1}|\}. \tag{11}$$

Note that, in Eqs. (8) and (10), we define the one-particle basis functions $\{|\eta_j\rangle\}$ and $\{\langle\phi_i|\}$. These functions will be referenced later on.

The intuition behind the subspaces W_{ket} and W_{bra} is that we sample the same basis functions for the *ket* and *bra* spaces from the inner grid points but different basis functions from the outer grid points. Over the outer grid points, we design the ket states to extend farther away from the scattering region than the bra states because we want to avoid surface effects at the edge of our grid. Because the kinetic energy operator T is nonlocal and, when written as $T=-\partial^2/\partial x^2$, the T operator acts directly on the ket space, stability requires that the ket vector space extends spatially beyond the bra space.

Now, solving the scattering problem is easy. First, we expand the scattered part of $|\Psi\rangle$ in W_{ket}:

$$|\Psi\rangle = |w_{\text{inc}}\rangle + \sum_j c_j|\eta_j\rangle \quad |\eta_j\rangle \in W_{\text{ket}}. \tag{12}$$

Second, we solve the Schrodinger equation by projection into the bra space, followed by matrix inversion (solving for the c_j variables):

$$\langle\phi_i|H - E_{\text{inc}}|\Psi\rangle = 0 \quad \text{where } \langle\phi_i| \in W_{\text{bra}}, \tag{13}$$

$$\sum_j \langle\phi_i|H - E_{\text{inc}}|\eta_j\rangle c_j = \langle\phi_i|H - E_{\text{inc}}|w_{\text{inc}}\rangle. \tag{14}$$

The reflected and transmitted coefficients are given by $c_{w_{\text{refl}}}$ and $c_{w_{\text{trans}}}$ in Eq. (12).

B. A steady state one electron formalism

It is important to realize that the procedure, Eqs. (12)–(14), for solving a time-independent scattering problem is not limited to genuine scattering situations and can be formulated as a steady-state problem which has source (i.e., incoming) and sink (outgoing) channels (see Ref. 1, Chap. 9). Formally, such a steady state problem is described in terms of the wave function:

$$|\Psi(t)\rangle = e^{-iE_{\text{inc}}t}|w_{\text{inc}}\rangle + \sum_j c_j(t)|\eta_j\rangle, \tag{15}$$

where $|w_{\text{inc}}\rangle$ drives the system with energy E_{inc}. The time-dependent Schrodinger equation gives us

$$H|\Psi\rangle = i\frac{\partial}{\partial t}|\Psi\rangle, \tag{16}$$

$$H\left(e^{-iE_{\text{inc}}t}|w_{\text{inc}}\rangle + \sum_j c_j(t)|\eta_j\rangle\right) = i\frac{\partial}{\partial t}\left(e^{-iE_{\text{inc}}t}|w_{\text{inc}}\rangle + \sum_j c_j(t)|\eta_j\rangle\right). \tag{17}$$

If we assume steady state, then $c_j(t)=c_j^0 e^{-iE_{\text{inc}}t}$ and Eq. (17) becomes

$$(H - E_{\text{inc}})\left(|w_{\text{inc}}\rangle + \sum_j c_j^0|\eta_j\rangle\right) = 0. \tag{18}$$

If we project again into the bra space, this is the same equation as Eq. (13). It should be emphasized, however, that a steady-state solution to Eq. (17) can be realized only provided that a sink channel is introduced through the boundary conditions. Such a sink can be implemented either by (i) imposing a suitable form of boundary wave function (as we have done by constructing $|w_{\text{refl}}\rangle$ and $|w_{\text{trans}}\rangle$ in Eqs. (4) and (5) or (ii) by applying appropriate absorbing boundary conditions, e.g., a surface self-energy term in the Hamiltonian.[20]

Author complimentary copy. Redistribution subject to AIP license or copyright, see http://jcp.aip.org/jcp/copyright.jsp

C. The two electrons and one bound state formalism

Consider now a two-electron Hamiltonian of the form

$$H(x_1,x_2) = T(x_1) + T(x_2) + V_{\text{ext}}(x_1) + V_{\text{ext}}(x_2) + W_{ee}(x_1,x_2). \tag{19}$$

Here T is the kinetic energy operator, V_{ext} is the fixed external potential acting on the electrons, and W_{ee} is the electron-electron interaction potential. We will assume that W_{ee} is nonzero only when both electrons are near the target. Such a situation is approximately realized in metal-insulator-metal junctions where screening in the metals makes it possible to model the space away from the junction as a free-electron system.

In order to generalize the formalism above to more than one electron (with one bound state in a quantum well), we first solve for the bound state of the one-electron Hamiltonian. Let us denote $|\chi_b^{\text{exact}}\rangle$ as the exact bound state of the one-electron Hamiltonian on an infinite grid, with spacing a:

$$|\chi_b^{\text{exact}}\rangle = \sum_{i=-\infty}^{\infty} b_i |g_i\rangle. \tag{20}$$

This defines the bound state in terms of an infinite array of numbers b.

For our calculations, we will need finite vectors representing the bound state in both the ket and bra spaces: To that end, we define

$$|\chi_b^{\text{ket},m}\rangle = \sum_{i=-m}^{m} b_i |g_i\rangle, \tag{21}$$

$$\langle\chi_b^{\text{bra},m}| = \sum_{i=-m}^{m} b_i \langle g_i|. \tag{22}$$

For m large enough, these finite vectors provide good approximations to the exact infinite bound-state wave functions. The needed length m will vary depending on the algorithm that we implement, but just as for the one-electron case, the ket vector should extend farther than the bra vector in order to avoid surface effects.

In order to solve for the two-electron wave function, the next step is to tensor together the appropriate single particle functions, creating two-electron functions, and then to construct the appropriate ket and bra spaces: $\widetilde{W_{\text{ket}}} = \text{span}\{\widetilde{|\eta_j\rangle}\}$ $\widetilde{W_{\text{bra}}} = \text{span}\{\widetilde{\langle\phi_i|}\}$ Here, we use tildes to signify two-electron states. Once we have specified the two-electron basis, we can solve the Schrodinger equation $H\widetilde{|\Psi\rangle} = E\widetilde{|\Psi\rangle}$ starting from an incoming state which acts as a driving force. Let $\widetilde{|\Psi\rangle} = \widetilde{|v_d\rangle} + \Sigma c_j \widetilde{|\eta_d\rangle}$. To compute the transmission of the incoming electron, we invert and solve for the c_j variables [just as in Eqs. (12)–(14)]:

$$\widetilde{\langle\phi_i|}H - E_{\text{inc}}\widetilde{|\Psi\rangle} = 0 \quad \widetilde{\langle\phi_i|} \in \widetilde{W_{\text{bra}}}, \tag{23}$$

$$\sum_j \widetilde{\langle\phi_i|}H - E_{\text{tot}}\widetilde{|\eta_j\rangle} c_j = -\widetilde{\langle\phi_i|}H - E_{\text{tot}}\widetilde{|v_d\rangle}. \tag{24}$$

In our model calculations, we assume that before the incoming electron arrives at the target, the bound electron is in the ground state of the target. Thus, the driving term $\widetilde{|v_d\rangle}$ is always one of the three options: $|w_{\text{inc}}\rangle \otimes |\chi_b^{\text{ket}}\rangle$ (distinguishable spinless particle) or $|w_{\text{inc}}\phi_b^{\text{ket}}\rangle$ (antisymmetrized indistinguishable same spin) or $|w_{\text{inc}}\bar{\phi}_b^{\text{ket}}\rangle$ (antisymmetrized, indistinguishable, opposite spin). Here, a bar denotes spin down, while no bar denotes spin up.

We now have the tools to solve the scattering problem within several different approximations, whereby we choose different forms for the incoming wave function and we select different ket and bra vector spaces. In what follows, we solve four distinct problems whereby one electron is transmitted through a target which is originally occupied by another electron.

1. The static approximation for spinless distinguishable particles or, equivalently, the static approximation for indistinguishable particles of opposite spin

The most elementary scattering algorithm invokes the static approximation, where we assume the particles are spinless and distinguishable and we ignore interparticle correlation. The incoming electron sees the average static field of the bound electron, while the bound electron may not respond to the incoming electron. The problem is nothing more than potential scattering, which is a one-particle problem. If we insist on using a two-particle formalism, then the two-particle wave function must consist of one particle frozen in a bound state. A sufficient two-particle basis is

$$\widetilde{W_{\text{ket}}} = \text{span}\{|\eta_j\rangle \otimes |\chi_b^{\text{ket},n}\rangle\}, \tag{25}$$

$$\widetilde{W_{\text{bra}}} = \text{span}\{\langle\phi_j| \otimes \langle\chi_b^{\text{bra},n-1}|\}. \tag{26}$$

Here, $|\eta_j\rangle$, $\langle\phi_j|$, and n were defined in Sec. II A, and our bound states extend into the outer grid points. As discussed above, the ket state extends farther than the bra state in order to avoid artificial effects on the grid surface.

Consider now the case of two electrons (or fermions) which are indistinguishable and have opposite spin. For concreteness, suppose that the bound-state electron is fixed with spin down and the incoming electron is always spin up. In this case, the two-electron wave function must be antisymmetrized, and the easiest way to accomplish that is to antisymmetrize the basis in Eqs. (25) and (26). We still insist on freezing the bound-state electron according to the static approximation, so the two-electron basis should be chosen as

$$\widetilde{W_{\text{ket}}} = \text{span}\{|\eta_j \bar{\chi}_b^{\text{ket},n}\rangle\}, \tag{27}$$

$$\widetilde{W_{\text{bra}}} = \text{span}\{\langle\phi_j \bar{\chi}_b^{\text{bra},n-1}|\}. \tag{28}$$

Here, we use the antisymmetrized notation: $|uv\rangle = |u\rangle \otimes |v\rangle - |v\rangle \otimes |u\rangle$.

If we compute the Hamiltonian matrix elements [according to Eq. (19)] for the basis vectors in Eqs. (25) and (26), we will find that the matrix elements are identical to the matrix elements for the basis vectors in Eqs. (27) and (28). The important observation is that, when the two electrons are

Author complimentary copy. Redistribution subject to AIP license or copyright, see http://jcp.aip.org/jcp/copyright.jsp

of opposite spin, the matrix elements of the electron-electron potential, $W_{ee}(x_1,x_2)$, are unchanged by introducing antisymmetry. More precisely, we assume here that W_{ee} is a function only of spatial coordinates, so that orbitals of opposite spin cannot be coupled together through W_{ee}. Thus, according to Eqs. (12)–(14), the two problems yield identical scattering solutions, and there is an isomorphism between the two situations. In what follows, we will refer to these situations equivalently as the "static approximation" or "static (opposite spin)," keeping in mind that this is a simple potential scattering problem.

2. The static exchange approximation or, more precisely, the static approximation for indistinguishable particles of the same spin

Next, consider the case of two (identical) electrons which are of the same spin where, just as before, one electron is initially bound to the target and the other electron is incoming. Equivalently, one can consider indistinguishable spinless particles, because spin is now irrelevant. According to the static approximation, we freeze one electron in the bound state and we solve for the scattering state of the other electron. In this case, there is no isomorphism between distinguishable (spinless) and indistinguishable (spin 1/2) problems. Indeed, the matrix elements of the electron-electron potential, $W_{ee}(x_1,x_2)$, are distinctly changed when we antisymmetrize the basis, going from basis elements like $|u\rangle\otimes|v\rangle$ to elements like $|uv\rangle$. The W_{ee} matrix elements introduce new ("exchange") terms in the effective Hamiltonian matrix, which are not zero because there is no spin orthogonality.

By analogy to the static approximation above, we might be tempted to choose for our basis:

$$\widetilde{W_{\text{ket}}} = \text{span}\{|\eta_j\chi_b^{\text{ket},n}\rangle\}, \tag{29}$$

$$\widetilde{W_{\text{bra}}} = \text{span}\{\langle\phi_j\chi_b^{\text{bra},n-1}|\}. \tag{30}$$

There is, however, a problem with this basis. The bra space is linearly dependent because $\langle\chi_b^{\text{bra},n-1}|$ is the sum of grid points from $(-n+1)a$ to $(n-1)a$, while the grid points $\langle\phi_j|$ also go from $(-n+1)a$ to $(n-1)a$. Because the two-electron basis is antisymmetrized, it follows that this two-electron basis is linearly dependent. This minor complication can be easily corrected, however, by allowing $\langle\chi_b^{\text{bra}}|$ to extend out one more grid space into the outer grid points. In other words, by extending the bra state from $\langle\chi_b^{\text{bra},n-1}|$ to $\langle\chi_b^{\text{bra},n}|$, we avoid linear dependence. Nevertheless, we still need the ket space to extend farther than the bra space, so all wave and bound basis elements in the ket space ($|\chi_b^{\text{ket}}\rangle$, $|w_{\text{inc}}\rangle$, $|w_{\text{refl}}\rangle$, and $|w_{\text{trans}}\rangle$) must also be extended uniformly. If we define extended three-point waves as

$$|w_{\text{refl}}^{(3)}\rangle \equiv |g_{-n+1}\rangle + e^{ika}|g_{-n}\rangle + e^{2ika}|g_{-n-1}\rangle, \tag{31}$$

$$|w_{\text{trans}}^{(3)}\rangle \equiv |g_{n-1}\rangle + e^{ika}|g_n\rangle + e^{2ika}|g_{n+1}\rangle, \tag{32}$$

then the correct two-electron basis in this situation is

$$\widetilde{W_{\text{ket}}} = \text{span}\{|w_{\text{refl}}^{(3)}\chi_b^{\text{ket},n+1}\rangle, |Y_{\text{inner}}\chi_b^{\text{ket},n+1}\rangle, |w_{\text{trans}}^{(3)}\chi_b^{\text{ket},n+1}\rangle\}, \tag{33}$$

$$\widetilde{W_{\text{bra}}} = \text{span}\{\langle\phi_j\chi_b^{\text{bra},n}|\}. \tag{34}$$

One can then invert the Schrodinger equation rigorously.

In what follows, this situation under the static approximation will be referred to as either the static exchange or static (same spin) case.

3. The fully correlated solution for nonidentical spinless particles or, equivalently, the fully correlated solution for identical particles of opposite spin

Consider again the case of nonidentical spinless particles. When we account for electronic correlation in the course of the scattering event, we allow for the bound electron and incoming electron to mutually respond to each other in the vicinity of the molecular target. To do that mathematically, we define $\tilde{A}$ as the subset of all pairs of inner grid points (corresponding to "closed channels"):

$$\tilde{A} = \text{span}\{|g_i\rangle\otimes|g_j\rangle\} \quad -n+2\le i, \quad j\le n-2. \tag{35}$$

For the case of nonidentical particles, we now choose our basis as follows:

$$\widetilde{W_{\text{ket}}} = \text{span}\left\{\begin{array}{c}\tilde{A}(\text{i.e., inner grid points})\\ |w_{\text{refl}}^{(3)}\rangle\otimes|\chi_b^{\text{ket},n+1}\rangle\\ |w_{\text{trans}}^{(3)}\rangle\otimes|\chi_b^{\text{ket},n+1}\rangle\\ |\chi_b^{\text{ket},n+1}\rangle\otimes|w_{\text{refl}}^{(3)}\rangle\\ |\chi_b^{\text{ket},n+1}\rangle\otimes|w_{\text{trans}}^{(3)}\rangle\end{array}\right\}, \tag{36}$$

Basis elements 2–5 represent the physical case where one electron is reflected or transmitted while a second electron is in a bound-state. These are the asymptotic possibilities for the two electrons in a multi-body scattering calculation.

The corresponding *bra*-space is obviously parallel:

$$\widetilde{W_{\text{bra}}} = \text{span}\left\{\begin{array}{c}\widetilde{A^\dagger}(\text{i.e. inner grid points})\\ \langle g_{-n+1}|\otimes\langle\chi_b^{\text{bra},n}|\\ \langle g_{n-1}|\otimes\langle\chi_b^{\text{bra},n}|\\ \langle\chi_b^{\text{bra},n}|\otimes\langle g_{-n+1}|\\ \langle\chi_b^{\text{bra},n}|\otimes\langle g_{n-1}|\end{array}\right\}. \tag{37}$$

Pictorially, the two-electron basis can be drawn as in Fig. 1. In this case, the extent of the bound-state orbital is not important computationally, provided that the ket basis elements extend farther out than the bra basis elements. This fundamental rule requires increasing the extent of bound states in coordination with the length of the incoming/reflected/transmitted waves.

Finally, note that if the Hamiltonian does not depend on spin, then understanding correlation for the case of distinguishable particles is equivalent to the case of indistinguishable particles with opposite spin. If we assume that the in-

Author complimentary copy. Redistribution subject to AIP license or copyright, see http://jcp.aip.org/jcp/copyright.jsp

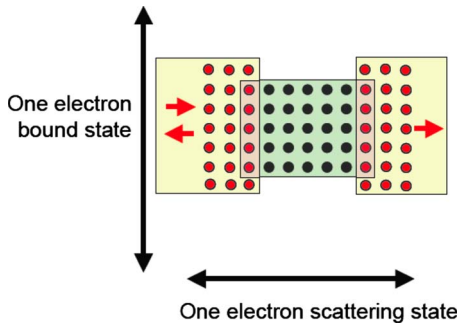

FIG. 1. (Color online) A graphical representation of our two-electron basis when correlation is included. The coordinate for particle one (incoming electron) is in the horizontal direction while the coordinate for particle two (bound electron) is in the vertical direction. The inner grid points are in the green region (in print, center panel with black circles). The reflected and transmitted waves (in the ket space) are red arrows, in the yellow regions (in print, light grey panels) to the left and right. These waves are tensored to the one-electron bound states. The bra space includes the bound states tensored to the grid points in the two smaller boxes around the inner grid points [colored pink (in print, dark grey with light grey circles)]. For the case of distinguishable spinless particles, we must include this diagram and the diagram which is rotated by 90° because, after collision, we do not know which particle will be ejected. For the case of indistinguishable particles of opposite spin, the same rules apply as before, only we must now reinterpret all two-particle basis elements as antisymmetrized products. For the case of indistinguishable particles of the same spin, this diagram is overcomplete, for we require only the upper left-hand triangle of the inner grid-point [green (in print, center panel with black circles)] region.

coming particle is spin up and the bound electron in the DBW is spin down, then the isomorphism is the simple mapping:

$$|u\rangle \otimes |v\rangle \rightarrow |u\bar{v}\rangle.$$

With this mapping, the two problems become entirely equivalent just as for the static approximation: all exchange terms are zero because of spin orthogonality. Thus, from now on, we will describe this situation equivalently as either "correlation (distinguishable)" or "correlation (opposite spin)."

4. The fully correlated solution for identical particles of the same spin

When we account for both correlation and exchange between electrons of the same spin, the only change we must make in the two-electron basis is to replace the direct products above with antisymmetric products, keeping in mind that antisymmetry now greatly reduces the number of degrees of freedom:

$$|u\rangle \otimes |v\rangle, |v\rangle \otimes |u\rangle \rightarrow |uv\rangle. \tag{38}$$

Thus, antisymmetry reduces the size of the two-electron basis roughly by a factor of 0.5. Otherwise, the formalism is exactly the same. From now on, this case will be abbreviated equivalently "exchange correlation" or "correlation (same spin)."

D. Multiple bound states

When we have multiple bound states, the formalism above for correlated solutions must be modified because we now have different channels, i.e., different outgoing waves, which are labeled according to the bound states to which they are attached (by conservation of energy). Let us use j to denote different channels corresponding to different bound-states. We then make the following replacements:

$$|w_{\mathrm{refl}}\rangle \rightarrow |w_{\mathrm{refl}}(j)\rangle,$$

$$|w_{\mathrm{trans}}\rangle \rightarrow |w_{\mathrm{trans}}(j)\rangle,$$

$$|\chi_b^{\mathrm{ket},m}\rangle \rightarrow |\chi_b^{\mathrm{ket},m}(j)\rangle.$$

In our basis $\widetilde{W_{\mathrm{ket}}}$, we couple waves from channel j only to bound states from channel j. We never mix the eigenfunctions from different channels, for energy conservation dictates the possible asymptotic forms of the wave function. Thus, for nonidentical spinless particles (or identical particles with opposite spin), each additional channel increases the size of the two-particle basis by only four functions. In the case of identical particles with the same spin, each additional channel increases the basis size by 2.

E. Two colliding scattering states

For completeness, we briefly discuss the case of two-electron tunneling, where two electrons enter the molecular target at nearly the same time and interact with each other, thus affecting the transmission and reflection of both. To the best of our knowledge, the effect of such processes on the overall tunneling current has not been estimated; however, the relevant transmission probability must be an essential ingredient in accurate calculations. Similarly, processes in which the incoming electron is large enough to make an ejection of a bound-state electron possible may also be important but pose similar mathematical difficulties.

While we have not addressed such processes in the present work, we expect that the multichannel method described in Sec. II D can be generalized to such situations by introducing a finite, discretely spaced, energy grid as an approximation to the continuum of possibilities for distributing the total energy between the two particles. We leave such a generalization to future work.

III. TWO ELECTRON RESULTS

We first apply this methodology to calculate electron transmission through a DBW that contains another bound electron, expanding on the work of Rejec *et al.*[17] Unlike the work of Rejec *et al.* who constructed triplet and singlet two-electron states from the start, we will assume that before the

Author complimentary copy. Redistribution subject to AIP license or copyright, see http://jcp.aip.org/jcp/copyright.jsp

collision there is no spin entanglement between the electrons. The following issues will be of interest:

(1) The effect of exchange and correlation on transmission as a function of energy.
(2) The effect of electron-electron repulsion, in particular, in the limit of strong repulsion. Here we will examine the effect of exchange and correlation on Coulomb blockade behavior.
(3) Inelastic transmission associated with transitions between electronic bound states in the DBW.

Second, for the case of a TBW, we will calculate the effect of electron-electron interactions on barrier crossings.

As a convenient DBW potential, we choose the following function specified by five parameters R_a, R_b, R_c, V_i, and V_o (Fig. 2):

$$V_{\text{ext}}(x) = \begin{cases} \frac{|V_o - V_i|}{2}\left(1 + erf\left(\frac{3(x-R_a)}{|R_a - R_b|}\right)\right) + V_i, & |x| < \frac{R_a + R_b}{2} \\ \frac{|V_o|}{2}\left(1 - erf\left(\frac{3(x-R_b)}{|R_b - R_c|}\right)\right), & \frac{R_a + R_b}{2} \le |x| < R_c \\ 0, & R_c \le |x|. \end{cases} \tag{39}$$

For the electron-electron potential, we choose

$$W_{\text{ee}}(x_1, x_2) = \begin{cases} W_0 e^{(x_1 - x_2)^2/2W_L}, & |x_1| \text{ and } |x_2| < \frac{R_a + R_b}{2} \\ 0, & |x_1| \text{ and/or } |x_2| > \frac{R_a + R_b}{2}. \end{cases} \tag{40}$$

Here, $[-(R_a+R_b/2),(R_a+R_b/2)]$ is the effective length of the double barrier and corresponds to the interval $[-10.5, 10.5]$ bohrs in Fig. 2. Electron-electron interactions are taken as nonzero only when both electrons are in this interval.

A. Resonance tunneling with one bound state

Figures 3 and 4 show the results of calculations done for electron tunneling through a DBW structure (in one dimension) that supports a single bound state. We examine two cases: relatively weak and relatively strong electron-electron coupling. Relatively weak coupling (Fig. 3) is defined such that two electrons of opposite spin can be bound in the DBW, while for relatively strong coupling (Fig. 4) such a doubly occupied state cannot be supported. Obviously, electrons with the same spin can never both be bound in the DBW due to the Pauli exclusion principle.

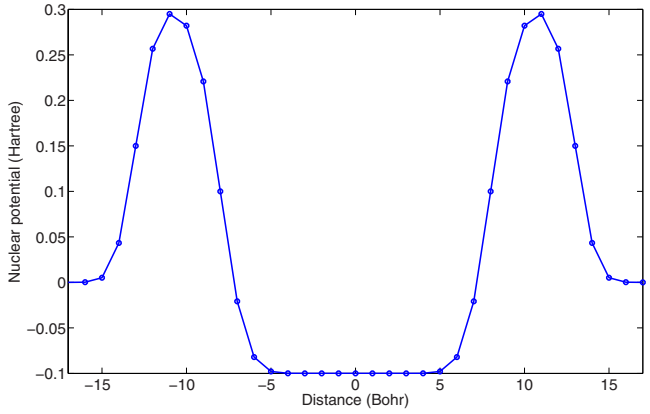

FIG. 2. (Color online) The double-barrier potential. In this figure, we choose R_a=8 bohrs, R_b=13 bohrs, R_c=17 bohrs, V_i=−0.1 hartree, V_o =0.3 hartree. Our grid spacing is a=1 bohr.

1. Weak electron-electron interaction energy

Figure 3 shows the energy dependent transmission in the weak coupling limit. The parameters used in the calculation are R_a=8 bohrs, R_b=13 bohrs, R_c=17 bohrs, V_i=−0.1 hartrees, V_o=0.3 hartrees, W_0=0.05 hartrees, and W_L=4 bohrs. See Eqs. (39) and (40) for details. The grid spacing in all our calculations here and below was taken as a=1 bohr. Shown are the results for the opposite-spin static approximation (red dashed line with stars) same-spin static approximation (blue dotted line with diamonds) opposite-spin correlated method (purple solid line), and same-spin correlated method (green dashed line with circles). Also shown is the case of noninteracting electrons, where the incoming electron does not see the bound electron at all (black solid line).

In the latter case of no electron-electron interaction, there is only one resonant tunneling peak, and the corresponding resonant tunneling state has a single node. This result follows because the nodeless state is the (occupied) bound state, and any one-electron resonant tunneling state must be orthogonal to the bound state. For a weak electron-electron repulsion energy, our well continues to allow only

Author complimentary copy. Redistribution subject to AIP license or copyright, see http://jcp.aip.org/jcp/copyright.jsp

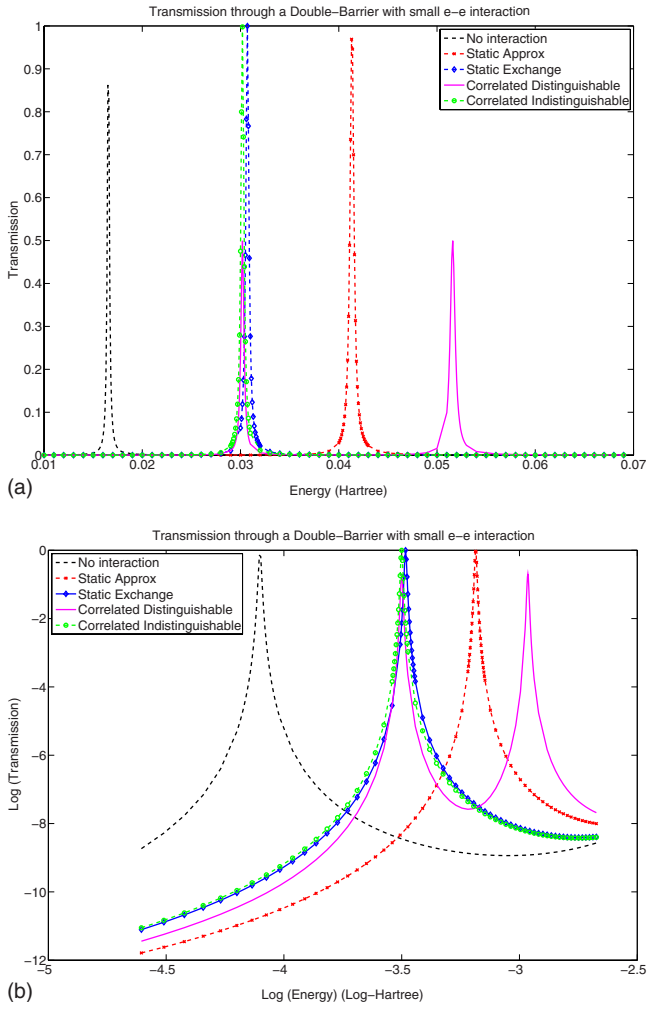

FIG. 3. (Color online) Resonant tunneling through a DBW with a weak electron-electron interaction energy. The parameters used in the calculation are $R_a=8$ bohrs, $R_b=13$ bohrs, $R_c=17$ bohrs, $V_i=-0.1$ hartree, $V_o=0.3$ hartree, $a=1$ bohr, $W_0=0.05$ hartree, and $W_L=4$ bohrs. See Eqs. (39) and (40) for details. We limit our incoming kinetic energy to 0.07 hartree because this is the ionization energy of the DBW. These two figures represent the same data on linear (a) and log scales (b).

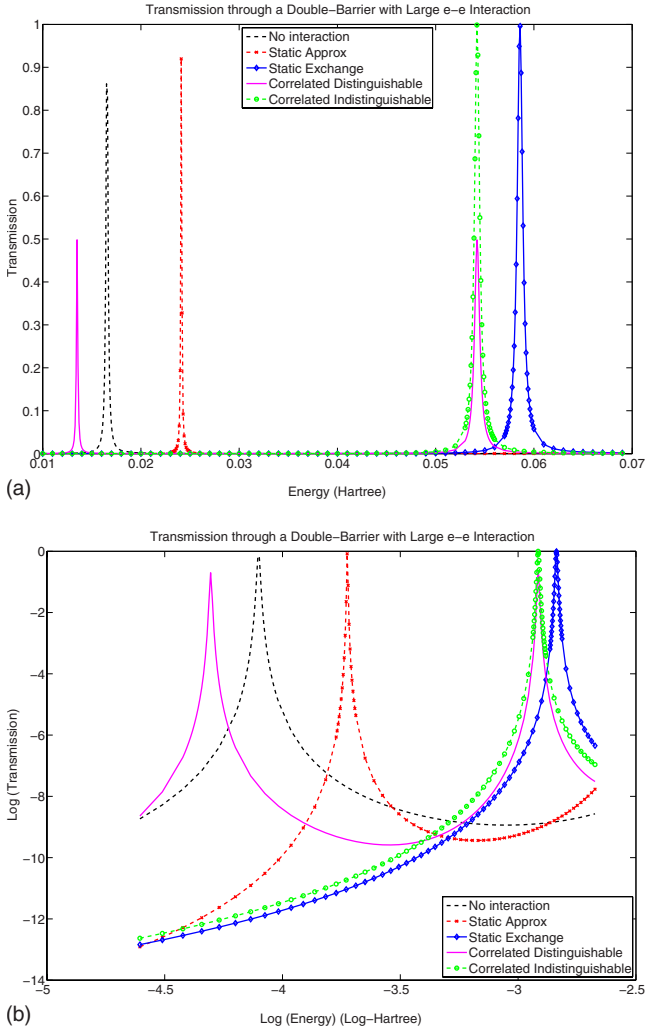

FIG. 4. (Color online) Resonant tunneling through a DBW with a strong electron-electron interaction energy. The parameters used in the calculation are $R_a=8$ bohrs, $R_b=13$ bohrs, $R_c=17$ bohrs, $V_i=-0.1$ hartree, $V_o=0.3$ hartree, $a=1$ bohr, $W_0=0.15$ hartree, and $W_L=4$ bohrs. See Eqs. (39) and (40) for details. We limit our incoming kinetic energy to 0.07 hartree because this is the ionization energy of the DBW. These two figures represent the same data on linear (a) and log scales (b).

one resonant tunneling peak (with one node) in both the static and static-exchange approximations. The static-exchange resonant energy does separate, however, from the potential scattering resonant energy. If we rationalize that that the resonant peaks occur at the energies of quasibound states, then the resonant energy of an antisymmetrized same-spin bound state should be lower because the exchange energy is always negative. Indeed, the static-exchange resonant peak is lower in energy than the potential scattering resonant peak.

Regarding the resonant tunneling energies computed with correlation effects, one finds that, for a weak e-e potential, the same-spin resonant tunneling peak lies very close to the static-exchange peak. Apparently, by insisting that the spatial part of the wave function be antisymmetric, the static-exchange approximation minimizes electron-electron repulsion, so that the effect of electron-electron correlation is not very strong.

The most interesting case is that of two electrons of opposite spin, when treated with correlation. Here, we find two peaks (in Fig. 3), each of height 0.5. The first peak (at 0.0302 hartree) has the asymptotic form

$$|\Psi_{\text{os},0.0302\ \text{hartree}}\rangle \tilde{\rightarrow} |w_{\text{inc}}\bar{\phi}_b\rangle + \frac{e^{i\theta}}{2}(|w_{\text{trans}}\bar{\phi}_b\rangle - |\phi_b\bar{w}_{\text{trans}}\rangle) + \frac{e^{i\theta'}}{2}(|w_{\text{refl}}\bar{\phi}_b\rangle + |\phi_b\bar{w}_{\text{refl}}\rangle), \quad (41)$$

$$\tilde{\rightarrow} |w_{\text{inc}}\bar{\phi}_b\rangle + \frac{e^{i\theta}}{2}(w_{\text{trans}}\phi_b - \phi_b w_{\text{trans}}) \otimes (\uparrow\downarrow + \downarrow\uparrow) + \frac{e^{i\theta'}}{2}(w_{\text{refl}}\phi_b + \phi_b w_{\text{refl}}) \otimes (\uparrow\downarrow - \downarrow\uparrow). \quad (42)$$

The peak at 0.0516 hartree has the asymptotic form:

Author complimentary copy. Redistribution subject to AIP license or copyright, see http://jcp.aip.org/jcp/copyright.jsp

$$|\Psi_{\text{os},0.0516\ \text{hartree}}\rangle$$

$$\tilde{\rightarrow}|w_{\text{inc}}\bar{\phi}_b\rangle + \frac{e^{i\theta}}{2}(|w_{\text{trans}}\bar{\phi}_b\rangle + |\phi_b\bar{w}_{\text{trans}}\rangle) + \frac{e^{i\theta'}}{2}(|w_{\text{refl}}\bar{\phi}_b\rangle - |\phi_b\bar{w}_{\text{refl}}\rangle) \quad (43)$$

$$\tilde{\rightarrow}|w_{\text{inc}}\bar{\phi}_b\rangle + \frac{e^{i\theta}}{2}(w_{\text{trans}}\phi_b + \phi_b w_{\text{trans}}) \otimes (\uparrow\downarrow - \downarrow\uparrow) + \frac{e^{i\theta'}}{2}(w_{\text{refl}}\phi_b - \phi_b w_{\text{refl}}) \otimes (\uparrow\downarrow + \downarrow\uparrow) \quad (44)$$

This result is easily understood from the work of Rejec *et al.*[17] Because we assume that the incoming electron is spin up and the target electron is spin down, the driving (incoming) term in our wave function is not an eigenvector of the S^2 operator. We can, however, decompose the driving term into singlet and triplet flavors:

$$|w_{\text{inc}}\bar{\phi}_b\rangle = \tfrac{1}{2}(w_{\text{inc}}\phi_b + \phi_b w_{\text{inc}}) \otimes (\uparrow\downarrow - \downarrow\uparrow) + \tfrac{1}{2}(w_{\text{inc}}\phi_b - \phi_b w_{\text{inc}}) \otimes (\uparrow\downarrow + \downarrow\uparrow). \quad (45)$$

Because the singlet and triplet states are mutually orthogonal and the Schrodinger equation is linear, we may propagate the scattering states of the singlet and triplet waves independently. The triplet state (for particles of opposite spin) will propagate exactly as for the triplet state (for particles of the same spin), for the spatial parts of both wave functions must be antisymmetric as a function of both electrons. This explains why one opposite-spin peak (of height 0.5 at roughly 0.0302 hartree) lies directly on top of the same-spin peak. The other peak (of height 0.5 at roughly 0.0516 hartree) corresponds to a spin singlet state, corresponding to symmetric spatial state for the two electrons, and this peak energy must be computed explicitly. Because of this decomposition, we find that for particles with opposite spin, at all resonant energies, one has equal probabilities for the spin-up or spin-down electron to come out of the well. There is no resonant peak at which only one spin comes out of the DBW, and there is no resonant peak of height 1 with only transmission. The case of opposite spins is thus very different from the case of same spins, as noted by Rejec *et al.*

One mystery remains, however, regarding the phase shift. According to our calculations, at the resonant transmission half-peaks, we have equal phase shifts $\theta \approx \theta'$ (to well within 0.05 rad) for the two outgoing (triplet and singlet) channels. This equality is not obvious according to a singlet-triplet decomposition. Rather, this equality at resonant peak energies suggests that, in the language of distinguishable particles, once the incoming particle has reached the target, one forgets which was originally the incoming particle and which was originally the bound-state particle: both particles are kicked out with equal probability and in both directions.

2. Strong electron-electron interaction energy

When the interaction energy is raised, all resonant transmission peaks are shifted up in energy. The relative positions of resonant tunneling peaks with one node do not change: The static-exchange peak is still lower in energy than the potential scattering peak (which is not shown because it is larger than the ionization energy of the DBW.) The same-spin correlation peak is still directly on top of one of the opposite-spin half-peaks (at 0.0547 hartree) as it must be. The opposite-spin half-peak at 0.0547 hartree still has the same asymptotic form as Eq. (42).

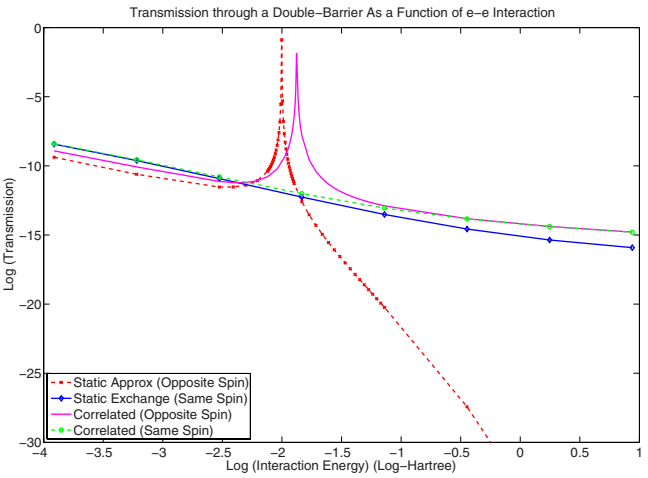

FIG. 5. (Color online) Transmission as a function of electron-electron repulsion W_0. Note that the transmission is much less asymptotically for the case of opposite-spin electrons when we ignore correlation. The DBW has the same parameters as in Figs. 3 and 4.

At low energies, however, we do see differences. For a strong electron-electron repulsion, we see a new peak in the potential scattering that corresponds to a quasibound state with no nodes. This is the potential scattering resonance peak at 0.024 hartree. For the case of correlated opposite-spin electrons (or, equivalently, distinguishable particles), there is also a narrow peak (with maximum transmission equal to 0.5) at 0.0135 hartree. Because these peaks correspond to resonance in a zero-node well state, and because the zero-node ground state is already occupied, we might expect these peaks to disappear when we antisymmetrize the wave function for same-spin electrons. Indeed, that is the case: we do not see any new same-spin peaks in Fig. 4. Finally, we mention that the half-peak at 0.0135 hartree has the same asymptotic form as Eq. (44).

B. Transmission as a function of electron-electron repulsion

In Fig. 5, we compute the transmission as a function of the electron-electron repulsion energy (W_0), when the incoming electron has energy 0.015 hartree. For small repulsion energies, we see peaks in the transmission profiles for the case of opposite-spin electrons. These are the peaks representing quasibound states with zero nodes discussed in Sec. III A 2. For large electron-electron repulsion energies, we enter the regime of the Coulomb blockade. First, for the case of opposite-spin electrons, we expect potential scattering to highly underestimate the transmission. According to potential scattering, the bound-state electron is fixed in its position, and the incoming electron can never push out the bound-state electron. If we allow for correlation, however,

Author complimentary copy. Redistribution subject to AIP license or copyright, see http://jcp.aip.org/jcp/copyright.jsp

we expect to see a small minimal current; for now there is a small probability that the incoming electron comes into the DBW and the bound-state electron goes out. This reasoning explains why the transmission calculated by potential scattering in Fig. 5 is so much smaller (asymptotically) than the transmission calculated for correlated opposite-spin electrons. Second, for the case of same-spin particles, the question of which electron comes in and which electron goes out is moot, and we see that the transmission curves for static exchange and correlation exchange are very similar to each other and to the case of opposite-spin electrons with correlation.

C. Transmission with two bound states

We now consider the multichannel problem, where the DBW can support two single-electron bound states of energy E_0 and E_1. However, because of the interelectronic energy (W_{ee}), both states cannot be occupied at the same time by any two electrons (irregardless of spin). We wish to investigate the behavior of the transmission as a function of energy near the excitation energy $E_{exc}=E_1-E_0$. If the kinetic energy of the incoming electron exceeds E_{exc}, the incoming electron can excite the bound-state electron from the ground state to the first excited state and then exit with a correspondingly smaller velocity. Although the effects of such phenomena on molecular conduction properties cannot be described within Landauer theory (especially for small voltage windows), the results shown below indicate the possible physical and computational signatures of such a transition. All data are presented in Fig. 6.

Our calculations find a transmission curve with a small kink where $E_{inc}=E_{exc}$. This becomes a large peak in the second derivative of the transmission (d^2T/dE^2), as shown. These findings are similar to inelastic tunneling spectra (IETSs) near the voltage where a vibrational mode may be excited. In the case of IETS, when a new channel for the incoming electron is opened, one finds a peak in the second derivative of the current-voltage curve, d^2I/dV^2. In our case, where the bound state is initially propelled into an excited state by the collision, note that the final outcome of the process could be photon emission, with the bound electron ultimately returning to the ground state. To examine this possibility computationally, we would need to include the interaction of electrons with the radiation field in the Hamiltonian.

D. The effect of electron-electron correlation on barrier crossings: The triple barrier well

In our final application, we consider the asymmetric triple-barrier well (TBW) potential shown in Fig. 7. This external potential admits two bound states, which are separated in space and shown in Fig. 7. A large barrier separates the ground state (on the left) and the first excited state (on the right) of the system. Nevertheless, these one-electron states are almost degenerate, separated by 0.013 hartree, and if the system exists in a fluctuating thermal environment, an electron on the left-hand side will occasionally transfer to the right hand side according to Marcus theory. This rate will be very small, however, because the barrier is large.

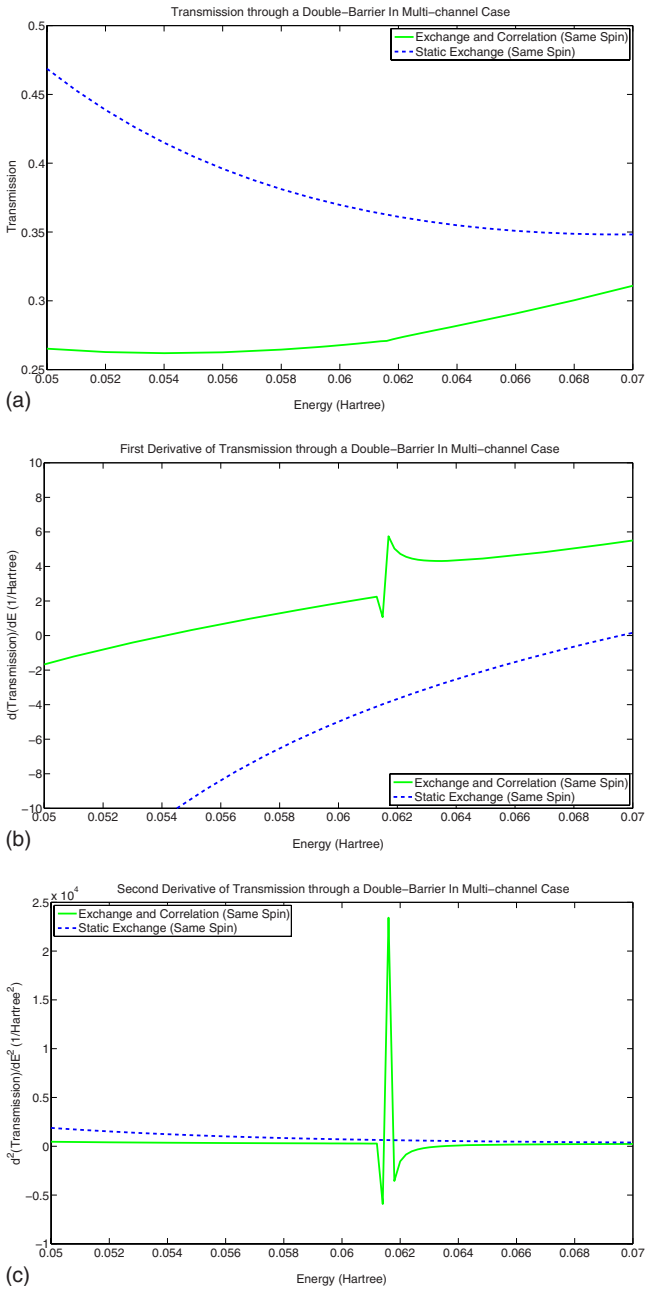

FIG. 6. (Color online) The transmission curve around the energy where $E_{inc}=E_{ex}$. Here, the DBW is parametrized by $R_a=8$ bohrs, $R_b=13$ bohrs, $R_c=17$ bohrs, $V_i=-0.1$ hartree, $V_o=0.05$ hartree, and $W_0=0.25$ hartree. (a) Function value, (b) first derivative, and (c) second derivative.

We now ask how this rate of transfer will be affected in the presence of a bath of free electrons, imagining that this electron transfer event may occur on a metal surface. Because the result is not very sensitive to spin, we focus on the two-electron opposite-spin case. We suppose that one spin-up electron is initially in the ground state on the left-hand side, and we plot the probability of transmission when there is another electron (spin-down) incoming from the left. We do this with and without accounting for correlation. Disregarding correlation, we first apply the static approximation, forcing the bound electron to remain fixed during the colli-

Author complimentary copy. Redistribution subject to AIP license or copyright, see http://jcp.aip.org/jcp/copyright.jsp

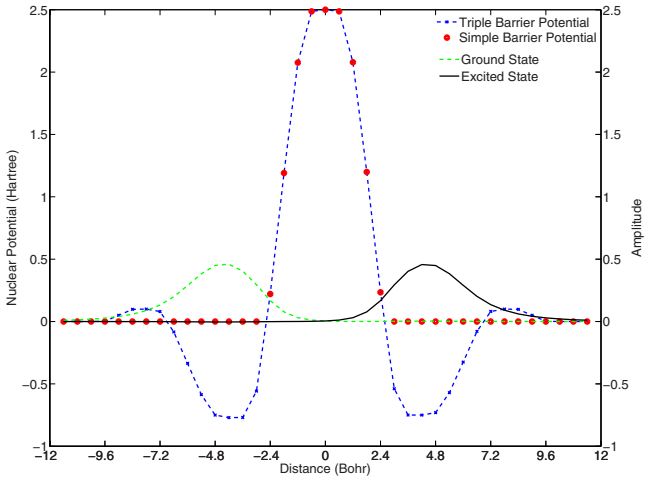

FIG. 7. (Color online) The geometry of a triple-barrier and simple-barrier external Hamiltonian. The triple-barrier external Hamiltonian is constructed by curvilinear extrapolation from the following (x,y) points: $(-10,0)$, $(-8,0.1)$, $(-4,-0.77)$, $(0,2.5)$, $(4,-0.75)$, $(8,0.1)$, and $(10,0)$. The slight asymmetry at $x=\pm 4$ gives us bound states which are on opposite sides of the barrier. The simple-barrier Hamiltonian has no wells next to the main central barrier.

sion; second, we solve for the correlated wave function, allowing the bound electron to respond to the incoming electron. We compare this transmission to the case of a simple-barrier potential (also shown in Fig. 7) where no trapped electron exists in the well. All results are shown in Fig. 8, where the (small) transmission is plotted in log format.

We find that, in the absence of a trapped electron, transmission is a rare event with probability roughly 10^{-6} both for a simple-barrier potential and an empty triple-barrier potential. Now, if there is a trapped electron on the left-hand side, but that electron is fixed in space (according to the static approximation) and acts only as a barrier to transmission, then the probability of transmission is immensely reduced (by five orders of magnitude) to approximately 10^{-11}. If, however, the trapped electron is allowed to respond to the incoming electron, then Fig. 8 shows that the transmission probability is only slightly reduced (to approximately 10^{-7}). This can be rationalized in terms of two competing forces.

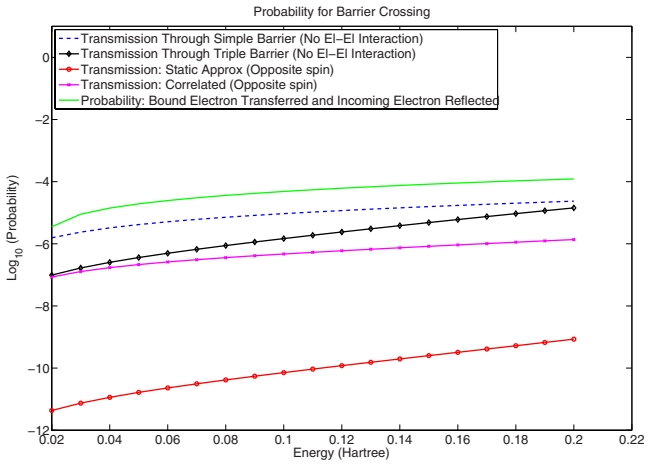

FIG. 8. (Color online) Transmission probabilities and electron transfer probabilities for the triple-barrier and simple-barrier Hamiltonian in Fig. 7.

On the one hand, as the incoming spin-down electron approaches the barrier, the trapped spin-up electron repels the incoming spin-up electron, thus acting to reduce transmission. On the other hand, the incoming spin-down electron also repels the spin-up trapped electron, pushing the spin-up electron forward, thus acting to increase transmission.

There is one final outcome that must be computed. As the incoming electron approaches the trapped electron, there is a finite probability that the incoming electron will impart enough momentum to force the trapped electron over the large middle barrier, while the incoming electron itself is reflected out of the system. Indeed, according to Fig. 8, this is the most probable form of barrier crossing, four times more likely than one-electron tunneling through the simple barrier. This effect may have ramifications for understanding electron transfer in a metallic environment.

IV. DISCUSSION

A. Summary

This article has presented an algorithm for computing the transmission of an electron through a molecular junction which is originally occupied by another electron. For the two-electron problem, the algorithm uses only grid points belonging to a finite grid. Ultimately, this is possible because we limit the kinetic energy operative to be a finite-difference operator, which implies, in the absence correlation, a tight-binding model. Whereas standard solid-state approaches for handling scattering states rely on complex self-energies at the boundaries, we avoid the self-energy entirely by using basis functions of "boundary waves" made up of two or three grid points. Just as self-energies depend on the energy of the individual electron near the boundary, so do the outgoing waves. Moreover, this method is applicable to the problem of a molecule between metal contacts, provided we can compute the band structure (eigenstates and eigenvalues) of the contact metal. In fact, using boundary waves or self-energies is entirely equivalent approach for treating the escape of a scattered electron from a boundary, though we find waves to be more intuitive in the case of a multichannel problem.

One encouraging result from our two-electron calculations is that, if one limits the region of the electron-electron interaction (which is physically motivated by screening outside the molecule), then one can also limit the size of our grid to be close to the boundaries of the molecular target and gain computational efficiency without losing much accuracy. Thus, even though the effects of electron-electron correlation on the wave function can be long range, far longer than the extent of electron-electron interaction, we find that this long-range behavior is not very important in our calculations. One easy check of the stability of our algorithm is to compute the transmission profile as we enlarge the grid region and change our approximation of the bound state. We find that, outside of the interaction region, if we increase the grid region, the transmission usually changes by at most 2%–3%.

Another measure of the stability of our algorithm is the degree to which it maintains charge conservation (i.e., the unitarity of the S-matrix). For the one channel problem, we find that the error in unitarity is near machine precision, sug-

Author complimentary copy. Redistribution subject to AIP license or copyright, see http://jcp.aip.org/jcp/copyright.jsp

gesting that our algorithm obeys a pseudovariational principle of some sort, which we have not yet found. For the multichannel problem, we find that the error in flux (i.e., the outgoing flux minus the incoming flux) is less than 1×10^{-5}, and this error decreases as we lengthen the grid region and we decrease the spacing between grid points. Last, we note that our algorithm is able to reproduce the deep tunneling regime (depending on grid size) for transmission rates smaller than 10^{-15}.

Finally, let us now detail the differences between our algorithm and the complex Kohn method. First, as published thus far, the complex Kohn method has not yet treated one-dimensional scattering with transmitted and reflected amplitudes, but rather it has focused on three-dimensional electron-molecule scattering and phase shifts. Second, because we make a finite approximation for the kinetic energy operator, we are able to compute scattering states over a finite grid rather than requiring scattering waves that go out to infinity. Third, by our choice of different ket and bra states, we naturally choose a nonsymmetric representation H of the Hamiltonian, and we must therefore invert a nonsymmetric matrix $(H-E)$ for the scattering solution. The complex Kohn method inverts a complex-symmetric (but not Hermitian) Hamiltonian operator $H-E$. Both algorithms are completely stable. (Notably, if one uses a Hermitian representation of the Hamiltonian operator, one ends up with a computationally unstable algorithm, which suffers from Kohn anomalies.[4]) In the future, it will be interesting to compare the computational efficiency of this algorithm versus the complex Kohn algorithm.

Regarding the effects of exchange and correlation, our general conclusions are in agreement with those reported by Rejec *et al.*[17] For same-spin electrons, enforcing exchange produces a nontrivial shift in the position of some resonance tunneling peaks (lowering their energy) while eliminating other resonant peaks entirely. This behavior is reasonable: enforcing exchange lowers the energy of the one-electron quasi-bound states, but it also forbids the same state to be doubly occupied according to the Pauli exclusion principle. Now, the correlation of same-spin electrons in a scattering apparatus also lowers the energy of quasibound states, only now these are two-electron quasibound states. This may explain, perhaps, why the correlation between same-spin electrons decreases the resonant transmission peak, though the effect is less dramatic than the exchange effect. Of course, as the electron-electron repulsion grows, we expect to see larger and larger effects of electron correlation (and we do).

For opposite-spin electrons, there is obviously no exchange effect, but the effects of correlation are significant. Whereas, initially, the incoming electron has spin up and the bound-state electron has spin down, this distinction is forgotten at resonance. For resonant energies, one has an equal chance of transmission or reflection, and the ejected electron can be either spin up or spin down. This symmetry will naturally be broken in the presence of magnetic fields but there remains the conclusion that complete resonant transmission (with probability 1) is impossible for electrons of opposite spin. Pure transmission is possible only when the incoming electron and the bound-state electron are spin entangled (as triplet or singlet) before impact, which seems unphysical.

Altogether, the results of our computations should give a straightforward and intuitive picture of how exchange and correlation affect the transmission profile for any given molecular target. First, exchange is crucial in the case of same-spin transmission. Second, correlation is crucial in the case of opposite-spin transmission, and less important in the case of same-spin transmission. We note that we have just reiterated the usual working philosophy of electronic structure theory when considering molecules in the gas phase. In that subdiscipline, the dominance of opposite-spin correlation effects over same-spin correlation effects has been well established, and recently, new correlation algorithms [e.g., SOS-MP2 (Ref. 21) and SCS-MP2 (Ref. 22)] have been developed which are devoted to focusing on the dominant opposite-spin correlation effects.

B. The 0.7 anomaly

In this paper, we have proposed an algorithm for solving an electron-scattering problem while properly taking into account the effects of electronic correlation. If we seek to transfer this algorithm to the problem of molecular conduction, however, our approach may be limited because we have modeled a molecule between two metals as one bound-state electron in a molecular target. For the case of real metal-molecule-metal junctions (at zero bias), such bound states may not exist, for all electronic orbitals on the molecule may hybridize to the continuum of states in the metallic leads. In that case, we must not think of bound states on molecules but rather quasibound states (with broadening) below the chemical potential.[23] Calculating electron transmission correctly, while accounting for electron-electron correlation, will be more difficult in such a case, as should be expected from any steady-state or time-independent approach.

Nevertheless, this basic scattering algorithm does capture some electron-correlation effects relevant to conduction experiments. In particular, as argued by Rejec *et al.*[17,24,25,27] and Flambaum and Kuchiev,[26] the 0.7 anomaly can be explained in terms of the resonant peaks shown in Fig. 4. The "0.7 anomaly"[18,23,28] in mesoscopic arises when one measures the electrical conductance through a quantum point contact (QPC) in the valley of a split voltage gate at temperatures between 1 and 4 K. For very large negative gate voltages, all electrons are excluded from the QPC and there is no current, but as the gate-voltage is raised, electrons flow into the channel and a current begins to flow. At very low temperatures, the conductance rises in steps of $G_0=2e^2/h$, the factor of 2 coming from spin degeneracy, as more and more transverse channels are allowed energetically.[29,30] There are, however, sometimes anomalies to this simple-step prediction, the most common anomaly being a small plateau in conductance near $0.7G_0$. Meir and co-workers[23,31,32] have argued that, near the 0.7 anomaly, there will be a quasibound state for only one electron (say, spin up) in the conduction channel. If this were true, one should consider spin up and spin down electrons approaching the channel where there is already another bound electron. Because the opposite-spin

Author complimentary copy. Redistribution subject to AIP license or copyright, see http://jcp.aip.org/jcp/copyright.jsp

case splits into peaks (triplet and singlet) of size 0.5, one of which exactly matches up with the same-spin peak of size 1 (a triplet), there may be conductance minijumps near $0.25G_0$ and $0.75G_0$, predictions which are, in fact, observed. See Ref. 17 for more details.

It is interesting to speculate on possible analogous effects of electronic correlation in molecular conduction. The spacing between energetic levels in molecules is much greater than the spacing in QPCs, so we see quantum effects in molecular conduction at room temperature, whereas these effects are washed away in QPCs above 5 K. Because electrons are able to better localize in molecules, we also expect to see sharp effects from electron-electron repulsion and correlation when measuring the conduction through molecules.

C. Theory: Extension to many electrons

In Sec. II, we presented an algorithm for computing the transmission of one electron traversing a one-dimensional target that contains another electron. We will now sketch how this algorithm can be extended to accommodate many electrons on a molecular target, anticipating that the computational cost should ideally scale quadratically with the number of electrons.

First, for real, three-dimensional molecular targets, we move from a basis of grid points to a basis of Gaussian orbitals centered on atomic nuclei. Second, recall that, for the two-electron DBW problem, we began the algorithm by calculating the ground state of the external potential, $|\phi_b\rangle$, which we took as the initial state for the bound electron. Similarly, for the n-body problem, we must calculate the ground-state wave function of the target molecule. For the moment, let us ignore ground-state correlation and assume that, initially, the target electrons on the molecule are in the mean-field Hartree–Fock (HF) ground state $|\phi_{\mathrm{HF}}\rangle$.

Third, we must specify an ansatz for the steady-state scattering wave function. For the two-electron problem, we constructed the exact ket form of the wave function as:

$$|\Psi_{\mathrm{HF}}\rangle = |w_{\mathrm{inc}}\phi_b\rangle + c_{\mathrm{refl}}|w_{\mathrm{refl}}\phi_b\rangle + c_{\mathrm{trans}}|w_{\mathrm{trans}}\phi_b\rangle + \sum_i c_i|g_i\phi_b\rangle, \tag{46}$$

$$|\Psi_{\mathrm{corr}}\rangle = |w_{\mathrm{inc}}\phi_b\rangle + c_{\mathrm{refl}}|w_{\mathrm{refl}}\phi_b\rangle + c_{\mathrm{trans}}|w_{\mathrm{trans}}\phi_b\rangle + \sum_{ij} c_{ij}|g_i g_j\rangle. \tag{47}$$

Analogously, we expect that the exact scattering state for the many-electron problem can be expanded in terms of the occupied $(ijkl)$ and virtual orbitals $(abcd)$ from the HF calculation, yielding an exponential number of variables to solve for

$$|\Psi_{\mathrm{HF}}\rangle = |w_{\mathrm{inc}}\phi_{\mathrm{HF}}\rangle + c_{\mathrm{refl}}|w_{\mathrm{refl}}\phi_{\mathrm{HF}}\rangle + c_{\mathrm{trans}}|w_{\mathrm{trans}}\phi_{\mathrm{HF}}\rangle + \sum_d t_d|d\phi_{\mathrm{HF}}\rangle, \tag{48}$$

$$|\Psi_{\mathrm{corr}}\rangle = |w_{\mathrm{inc}}\phi_{\mathrm{HF}}\rangle + c_{\mathrm{refl}}|w_{\mathrm{refl}}\phi_{\mathrm{HF}}\rangle + c_{\mathrm{trans}}|w_{\mathrm{trans}}\phi_{\mathrm{HF}}\rangle + \sum_d t_d|d\phi_{\mathrm{HF}}\rangle + \sum_{iad} t_i^a(d)|d\phi_i^a\rangle + \sum_{ijabd} t_{ij}^{ab}(d)|d\phi_{ij}^{ab}\rangle + \sum_{ijkabcd} t_{ijk}^{abc}(d)|d\phi_{ijk}^{abc}\rangle + \ldots. \tag{49}$$

Here d is a virtual orbital capturing the path of the incoming scattering electron. Although the ansatz [Eq. (49)] is intractable computationally, we can estimate the exact solution by means of an approximate solution that limits the number of variables to single and double excitations:

$$|\Psi_{\mathrm{double}}\rangle = |w_{\mathrm{inc}}\phi_{\mathrm{HF}}\rangle + c_{\mathrm{refl}}|w_{\mathrm{refl}}\phi_{\mathrm{HF}}\rangle + c_{\mathrm{trans}}|w_{\mathrm{trans}}\phi_{\mathrm{HF}}\rangle + \sum_d t_d|d\phi_{\mathrm{HF}}\rangle + \sum_{iad} t_i^a(d)|d\phi_i^a\rangle + \sum_{ijabd} t_{ij}^{ab}(d)|d\phi_{ij}^{ab}\rangle. \tag{50}$$

Physically, the term $\Sigma_{iad}t_i^a(d)|d\phi_i^a\rangle$ in Eq. (50) captures the response of a target electron (i) to the incoming electron (d), i.e., it allows for one-electron excitation $(i\rightarrow a)$. The term $\Sigma_{ijabd}t_{ij}^{ab}(d)|d\phi_{ij}^{ab}\rangle$ allows both for (i) the incoming electron to excite two electrons $(ij\rightarrow ab)$ and (ii) the incoming electron to excite one target electron which excites another target electron, which will be important for closed shell molecules, where alpha and beta electrons are paired together. Last, if one wants to account for some electronic correlation within the initial and final asymptotic states of the target electrons, one can simply replace $|\phi_{\mathrm{HF}}\rangle$ by a correlated ground-state wave function $|\phi_{\mathrm{corr}}\rangle$ in the first three terms on the right hand side of Eq. (50).

While the ansatz in Eq. (50) may not at first appear similar to that in Eq. (47), we can construct a very clear analogy by changing our basis from canonical molecular orbitals to a set of *localized* occupied $(ijkl)$ and virtual orbitals $(abcd)$ (corresponding to bonding and antibonding orbitals), and then recognizing that a localized orbital is equivalent to a grid point in this formulation. Furthermore, in such a localized orbital basis, we may borrow from the techniques of local correlation theory and quantum chemistry, insisting that orbitals $iajb$ be close together. Thus, even though the largest tensor $(t_{ij}^{ab}(d))$ in Eq. (50) has five indices, we should be able reduce the number of variables in the wave function to be quadratic. Note that we can never make any assumptions concerning the locality of the virtual orbital d relative to orbitals $iajb$. The orbitals labeled d represent the scattering electron that traverses the entire molecule and thus they overlap with every orbital in the set $iajb$. Unlike the ground-state problem, where local correlation theory can be successfully applied to a linear number of variables, the dynamical scattering problem admits no fewer than a quadratic number of variables.

Finally, we note that for a short-ranged electron-electron potential (with screening far away from the molecule), the Hamiltonian matrix $(H-E)$ should have only a quadratic number of significant matrix elements in a localized basis. Thus, $(H-E)$ should be a very sparse matrix with a quadratic

Author complimentary copy. Redistribution subject to AIP license or copyright, see http://jcp.aip.org/jcp/copyright.jsp

number of nonzero elements, and provided that the non-Hermitian matrix can be inverted by an iterative algorithm, the computational time for solving the scattering problem should scale quadratically with the size of the system.

V. CONCLUSIONS

This article has described a new method for treating the effects of exchange and correlation on electron transmission through a molecular target. We have implemented the algorithm for the case of an electron transmitted through a molecular target containing another electron. For same-spin electrons, we find that exchange is crucial, strongly shifting downward the position of the resonance tunneling peak, depending on the strength of the electron-electron repulsion (W_0). The effect of correlation on top of exchange is more modest but also produces a shift depending on W_0. For opposite-spin electrons, there is obviously no exchange effect, but the effect of correlation is enormous, splitting full peaks into half-peaks and forcing the outgoing state into a spin-singlet or a spin-triplet configuration. When the electron-electron repulsion energy is very large, we find that there is a small transmission which comes about when the first incoming electron jumps into the bound-state and the second bound-state electron comes out. This phenomenon can be correctly described if we account for electronic correlation or if we consider the static-exchange approximation for same-spin electrons; potential scattering drastically underestimates the amount of transmission as the e-e repulsion energy grows larger. Finally, we have shown that when a new channel is introduced, the conductance shows a peak in the second derivative of transmission with respect to energy. Taken together, these results should yield some information as to what is the general effect of exchange and correlation in molecular conduction, where few such rigorous calculations have yet been made. In the future, for the many-electron scattering problem, the full algorithm detailed in Sec. IV C should be implemented. For the conduction problem, however, the question remains as to how we may account for the broadening of the molecular levels (by contact to the metal) in a many-body scattering algorithm in order to correctly account for electron-electron correlation.

ACKNOWLEDGMENTS

We thank Bill Miller, Tomaž Rejec, Yigal Meir, Kieron Burke, and Martin Head-Gordon for helpful discussions and references. This work was supported by the U.S. Israel Binational Science Foundation, the German-Israel Foundation, and the Israel Science Foundation. J.E.S. was supported the by NSF International Research Fellowship Program.

[1] A. Nitzan, *Chemical Dynamics in Condensed Phases* (Oxford University Press, New York, 2006).
[2] S. Datta, *Electronic Transport in Mesoscopic Systems* (Cambridge University Press, Cambridge, England, 1995).
[3] W. Kohn, Phys. Rev. **74**, 1763 (1948).
[4] J. Z. H. Zhang, S. Chu, and W. H. Miller, J. Chem. Phys. **88**, 6233 (1988).
[5] T. N. Rescigno, B. H. Lengsfield, and C. W. McCurdy, in *Modern Electronic Structure Theory*, edited by D. Yarkony (World Scientific, New Jersey, 1995), Vol. I, p. 501.
[6] C. Winstead and V. McKoy, in *Modern Electronic Structure Theory*, edited by D. Yarkony (World Scientific, New Jersey, 1995), Vol. II, p. 1375.
[7] D. J. Zvijac, E. J. Heller, and J. C. Light, J. Phys. B **8**, 1016 (1975).
[8] P. S. Krstic, D. J. Dean, X. G. Zhang, D. Keffer, Y. S. Leng, P. T. Cummings, and J. C. Wells, Comput. Mater. Sci. **28**, 321 (2003).
[9] Y. Dahnovsky, V. G. Zakrzewski, A. Kletsov, and J. V. Ortiz, J. Chem. Phys. **123**, 184711 (2005).
[10] Y. Dahnovsky and J. V. Ortiz, J. Chem. Phys. **124**, 144114 (2006).
[11] A. Ferretti, A. Calzolari, R. D. Felice, and F. Manghi, Phys. Rev. B **72**, 125114 (2005).
[12] A. Ferretti, A. Calzolari, R. D. Felice, F. Manghi, M. J. Caldas, M. B. Nardelli, and E. Molinari, Phys. Rev. Lett. **94**, 116802 (2005).
[13] V. Meden, T. Enss, S. Andergassen, W. Metzner, and K. Schonhammer, Phys. Rev. B **71**, 041302 (2005).
[14] X. Barnabe-Theriault, A. Sedeki, V. Meden, and K. Schonhammer, Phys. Rev. B **71**, 205327 (2005).
[15] V. Meden and F. Marquardt, Phys. Rev. Lett. **96**, 146801 (2006).
[16] P. Delaney and J. C. Greer, Phys. Rev. Lett. **93**, 036805 (2004).
[17] T. Rejec, T. Ramšak, and J. H. Jefferson, Phys. Rev. B **67**, 075311 (2003).
[18] S. M. Cronenwett, H. Lynch, D. Goldhaber-Gordon, L. Kouwenhoven, C. M. Marcus, K. Hirose, N. S. Wingreen, and V. Umansky, Phys. Rev. Lett. **88**, 226805 (2002).
[19] S. Saebo and P. Pulay, Annu. Rev. Phys. Chem. **44**, 213 (1993).
[20] M. Galperin, S. Toledo, and A. Nitzan, J. Chem. Phys. **117**, 10817 (2002).
[21] Y. Jung, R. Lochan, A. Dutoi, and M. Head-Gordon, J. Chem. Phys. **121**, 9793 (2004).
[22] S. Grimme, J. Chem. Phys. **118**, 9095 (2003).
[23] T. Rejec and Y. Meir, Nature (London) **442**, 900 (2006).
[24] T. Rejec, T. Ramšak, and J. H. Jefferson, Phys. Rev. B **62**, 12985 (2000).
[25] T. Rejec, T. Ramšak, and J. H. Jefferson, J. Phys.: Condens. Matter **12**, L233 (2000).
[26] V. V. Flambaum and M. Y. Kuchiev, Phys. Rev. B **61**, R7869 (2000).
[27] T. Rejec, T. Ramšak, and J. H. Jefferson, Phys. Rev. B **65**, 235301 (2002).
[28] Y. Meir, J. Phys.: Condens. Matter **20**, 164208 (2008).
[29] B. J. van Wees, H. van Houten, C. W. J. Beenakker, J. G. Williamson, L. P. Kouwenhoven, D. van der Marel, and C. T. Foxon, Phys. Rev. Lett. **60**, 848 (1988).
[30] D. A. Wharam, T. J. Thornton, R. Newbury, M. Pepper, H. Ahmed, J. E. F. Frost, D. G. Frost, D. G. Hasko, D. C. Peacock, D. A. Ritchie, G. A. C. Jones, J. Phys. C **21**, L209 (1988).
[31] K. Hirose, Y. Meir, and N. Wingreen, Phys. Rev. Lett. **90**, 026804 (2003).
[32] Y. Meir, K. Hirose, and N. Wingreen, Phys. Rev. Lett. **89**, 196802 (2002).

Author complimentary copy. Redistribution subject to AIP license or copyright, see http://jcp.aip.org/jcp/copyright.jsp